Deeply Virtual Compton Scattering in Hall A with CEBAF at 12 GeV

Carlos Muñoz Camacho

Los Alamos National Laboratory, Los Alamos, NM 87545

JLab PAC 30
Aug 21-25, 2006

Collaboration

- Ohio University (J. Roche)
- Old Dominion University (C. E. Hyde-Wright)
- CEA/DAPNIA & CNRS/IN2P3 (B. Michel)
- Los Alamos National Laboratory (C. Muñoz Camacho)
- Jefferson Lab
- Florida International University
- Massachusetts Institute of Technology
- Rutgers University
- Stony Brook University
- University of Virginia
- Seoul National University
- University of Ljubljana

(Hall A Collaboration proposal)

DVCS ($\gamma^* p \to \gamma\, p$)

DVCS through its φ−dependence
and its interference with BH
provides a rich and clean survey of
GPDs and GPD integrals

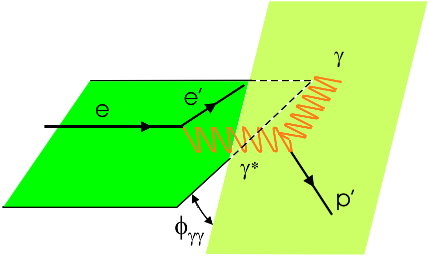

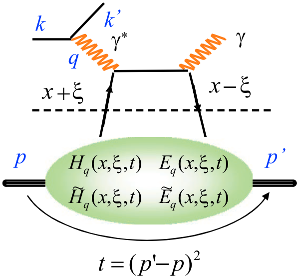

Bjorken limit

$$Q^2 \gg \Lambda_{\text{QCD}}$$
$$t \ll Q^2$$

$x \pm \xi$: momentum fraction
$t_{\text{min}} - t$: Fourier conjugate to transverse position of parton in nucleon

Interference with Bethe-Heitler (BH)

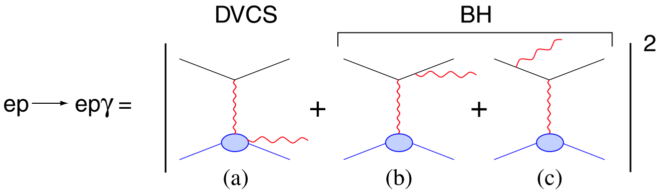

$$\mathcal{T}^2 = |\mathcal{T}_{BH}|^2 + \mathcal{I} + |\mathcal{T}_{DVCS}|^2$$

$\mathcal{T}_{BH}$: independent of helicity,
and *exactly known* up to form factors accuracy in our $-t$ range ($< 1\,\mathrm{GeV}^2$)

$$\frac{d\sigma}{d\Phi} = \frac{d\sigma_{BH}}{d\Phi} + \frac{d\sigma_{\mathrm{Int}}}{d\Phi} + \frac{d\sigma_{DVCS}}{d\Phi}$$

Cross section measurements:
Separation of $\Im$m and $\Re$e parts of DVCS observables

1.- Helicity-correlated cross section: $\Im$maginary part

$$\frac{d^5\Sigma}{d^5\Phi} = \frac{1}{2}\left[\frac{d^5\sigma^+}{d^5\Phi} + \frac{d^5\sigma^-}{d^5\Phi}\right] =$$

$$\underbrace{\sin(\phi_{\gamma\gamma})\Gamma_1^{\Im}\,\Im\text{m}\left[\mathcal{C}^I(\mathcal{F})\right] - \sin(2\phi_{\gamma\gamma})\Gamma_2^{\Im}\,\Im\text{m}\left[\mathcal{C}^I(\mathcal{F}^{\text{eff}})\right]}_{\text{Interference BH-DVCS}} + \underbrace{\sin(\phi_{\gamma\gamma})\Gamma_1^{\Im}\eta_{s1}\Im\text{m}\left[\mathcal{C}^{\text{DVCS}}(\mathcal{F}^{\text{eff}},\mathcal{F}^*)\right]}_{|\text{DVCS}|^2\text{ (twist-3)}}$$

- Different $\phi_{\gamma\gamma}$ dependence of Twist-2 & Twist-3 interference terms:
  $\Rightarrow$ *independent determination*
- $\sin\phi_{\gamma\gamma}\Gamma_1^{\Im}$ term determines observable $\Im\text{m}\left[\mathcal{C}^{I,\text{exp}}(\mathcal{F})\right]$:

$$\Im\text{m}\left[\mathcal{C}^{I,\text{exp}}(\mathcal{F})\right] = \Im\text{m}\left[\mathcal{C}^I(\mathcal{F})\right] + \langle\eta_{s1}\rangle\Im\text{m}\left[\mathcal{C}^{\text{DVCS}}(\mathcal{F}^{\text{eff}},\mathcal{F}^*)\right] \qquad |\langle\eta_{s1}\rangle|_{E00-110} < 0.01$$

Cross section measurements: Separation of $\Im$m and $\Re$e parts of DVCS observables

2.- Helicity-independent cross section: $\Re$eal part

$$\frac{d^5\sigma}{d^5\Phi} = \frac{1}{2}\left[\frac{d^5\sigma^+}{d^5\Phi} + \frac{d^5\sigma^-}{d^5\Phi}\right] = \underbrace{\frac{d^5\sigma(|BH|^2)}{d^5\Phi}}_{\text{Known from FF}} + \underbrace{\Gamma\,\eta\,\mathcal{C}^{\text{DVCS}}(\mathcal{F},\mathcal{F}^*)}_{|\text{DVCS}|^2\ \text{(twist-2)}} +$$

$$\underbrace{(\Gamma_0^{\Re} - \cos(\phi_{\gamma\gamma})\Gamma_1^{\Re})\Re\text{e}\left[\mathcal{C}^I(\mathcal{F})\right] + \Gamma_{0,\Delta}^{\Re}\Re\text{e}\left[\mathcal{C}^I + \Delta\mathcal{C}^I\right](\mathcal{F}) + \cos(2\phi_{\gamma\gamma})\Gamma_2^{\Re}\Re\text{e}\left[\mathcal{C}^I(\mathcal{F}^{\text{eff}})\right]}_{\text{Interference BH-DVCS}}$$

- $\Re\text{e}\left[\mathcal{C}^{I,\,\text{exp}}(\mathcal{F})\right] = \Re\text{e}\left[\mathcal{C}^I(\mathcal{F})\right] + \langle\eta_{c1}\rangle\,\mathcal{C}^{\text{DVCS}}(\mathcal{F},\mathcal{F}^*)$
- $\Re\text{e}\left[\mathcal{C}^{I,\,\text{exp}} + \Delta\mathcal{C}^{I,\,\text{exp}}\right](\mathcal{F}) = \Re\text{e}\left[\mathcal{C}^I + \Delta\mathcal{C}^I\right](\mathcal{F}) + \langle\eta_0\rangle\,\mathcal{C}^{\text{DVCS}}(\mathcal{F},\mathcal{F}^*)$

$$|\langle\eta_{0,c1}\rangle|_{E00-110} < 0.05$$

From cross sections to Compton Form Factors ($\mathcal{F}$)

$$\mathcal{F} = \{\mathcal{H}, \tilde{\mathcal{H}}, \mathcal{E}, \tilde{\mathcal{E}}\}$$

Twist 2:

$$\mathcal{C}^I(\mathcal{F}) = F_1(t)\mathcal{H}(\xi,t) + \xi G_M(t)\tilde{\mathcal{H}}(\xi,t) - \frac{t}{4M^2}F_2(t)\mathcal{E}(\xi,t)$$

$$\left[\mathcal{C}^I + \Delta\mathcal{C}^I\right](\mathcal{F}) = F_1(t)\mathcal{H}(\xi,t) - \frac{t}{4M^2}F_2(t)\mathcal{E}(\xi,t) - \xi^2 G_M(t)\left[\mathcal{H}(\xi,t) + \mathcal{E}(\xi,t)\right]$$

$$\mathcal{C}^{\text{DVCS}}(\mathcal{F},\mathcal{F}^*) = (1-\xi^2)\left[\mathcal{H}(\xi,t)\mathcal{H}^*(\xi,t) + \tilde{\mathcal{H}}(\xi,t)\tilde{\mathcal{H}}^*(\xi,t)\right] + \ldots$$

Twist 3:

$$\mathcal{C}^I(\mathcal{F}^{\text{eff}}) = F_1(t)\mathcal{H}^{\text{eff}}(\xi,t) + \xi G_M(t)\tilde{\mathcal{H}}^{\text{eff}}(\xi,t) - \frac{t}{4M^2}F_2(t)\mathcal{E}^{\text{eff}}(\xi,t)$$

$$\mathcal{C}^{\text{DVCS}}(\mathcal{F}^{\text{eff}},\mathcal{F}^*) = (1-\xi^2)\left[\mathcal{H}^{\text{eff}}(\xi,t)\mathcal{H}^*(\xi,t) + \tilde{\mathcal{H}}^{\text{eff}}(\xi,t)\tilde{\mathcal{H}}^*(\xi,t)\right] + \ldots$$

($F_1(t)$, $F_2(t)$, with $-t \ll Q^2$)

Cross section measurements

Cross sections give INDEPENDENT sensitivity
to $\Re$eal and $\Im$maginary parts of (combinations of) Compton form factors

$$\mathcal{H}(\xi,t) = \sum_f e_f^2 \left\{ i \underbrace{\pi \left[H_f(\xi,\xi,t) - H_f(-\xi,\xi,t) \right]}_{\Im\text{maginary part } (x=\pm\xi)} + \underbrace{\mathcal{P}\int_{-1}^{+1} dx \left[\frac{1}{\xi - x} - \frac{1}{\xi + x} \right] H_f(x,\xi,t)}_{\Re\text{eal part}} \right\}$$

Missing mass squared $e\ p \rightarrow e\ \gamma\ X$ (E00-110)

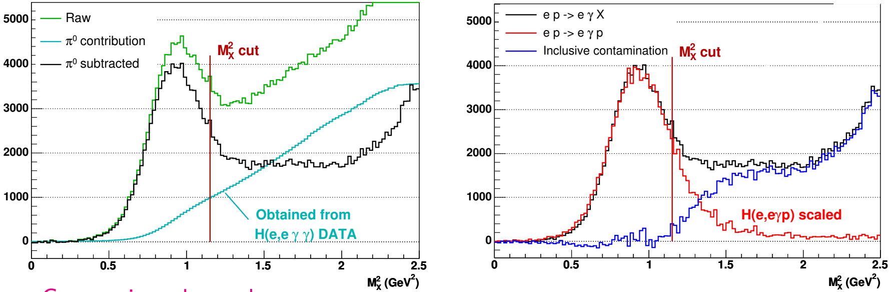

Competing channels:

- π^0 electroproduction: $e\ p \rightarrow e\ p\ \pi^0 X \rightarrow e\ p\ \gamma\ \gamma\ X$
- Associated DVCS: $e\ p \rightarrow e\ N\ \pi\ \gamma$
  - Non-resonant: $e\ p \rightarrow e\ N\ \pi\ \gamma$ $\quad M_X^2 > (M + m_{\pi^0})^2$
  - Resonant: $e\ p \rightarrow e\ (\Delta$ or $N^*)\gamma$ $\quad m_\Delta^2 = 1.52$ GeV^2

DVCS cross sections (E00-110)

Accurate determination of $\phi_{\gamma\gamma}$ dependence of $d\Sigma = \dfrac{\sigma^{\rightarrow} - \sigma^{\leftarrow}}{2}$ and $d\sigma = \dfrac{\sigma^{\rightarrow} + \sigma^{\leftarrow}}{2}$

$Q^2 = 2.3\,\text{GeV}^2, \ \langle t \rangle = -0.28\,\text{GeV}^2, \ x_{\text{Bj}} = 0.36$

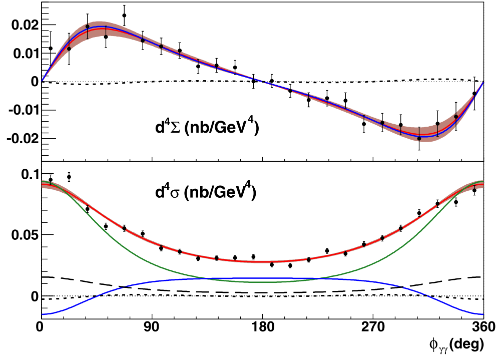

— $\Im\text{m}\, \mathcal{C}^{\mathcal{I},\text{exp}}(\mathcal{F})$
⋯ $\Im\text{m}\, \mathcal{C}^{\mathcal{I}}(\mathcal{F}^{\text{eff}})$
} *1 free parameter each*

— Total fit

— $\Re\text{e}\, \mathcal{C}^{\mathcal{I},\text{exp}}(\mathcal{F})$
- - - $\Re\text{e}\, [\mathcal{C}^{\mathcal{I}} + \Delta\mathcal{C}^{\mathcal{I}}]^{\text{exp}}(\mathcal{F})$
⋯ $\Re\text{e}\, \mathcal{C}^{\mathcal{I}}(\mathcal{F}^{\text{eff}})$
} *1 free parameter each*

— Bethe-Heitler *fixed*

— Total fit

$d\sigma$: - rich and complex $\phi_{\gamma\gamma}$ structure beyond BH
- interesting & complementary GPD information (real part)

Q^2-dependence: twist-2 dominance

$\Im\mathrm{m}\,\mathcal{C}^{\mathcal{I}}(\mathcal{F})$

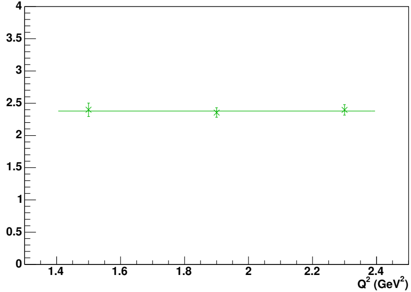

$\Im\mathrm{m}\,\mathcal{C}^{\mathcal{I}}(\mathcal{F}^{\mathrm{eff}})$

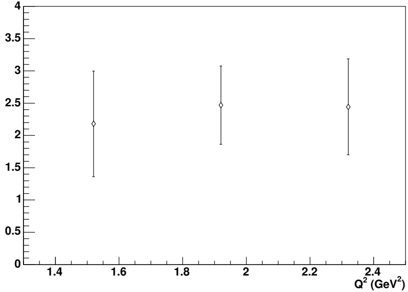

Larger Q^2 range for this proposal (2:1 for $Q^2 > 2\,\mathrm{GeV}^2$) will provide:

- Accurate estimate of twist-2 dominance
- Better determination of higher twists

GPD linear combinations and integrals

E00-110 results

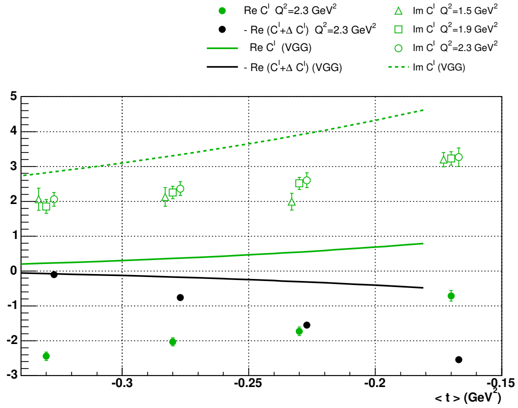

- $t-$distributions at *one* $x_{\text{Bj}} = 0.36$
- Q^2-dependence only in $\Im$m part

New experiment

- Wide range on :
  - $0.36 < x_{\text{Bj}} < 0.6$
  - $3\,\text{GeV}^2 < Q^2 < 9\,\text{GeV}^2$
- High statistics
  $t-$dependence at each x_{Bj} and Q^2
- Strong test of factorization at each (x_{Bj}, t)

Kinematic coverage

JLab12 with 3, 4, 5 pass beam
(6.6, 8.8, 11.0 GeV beam energy)

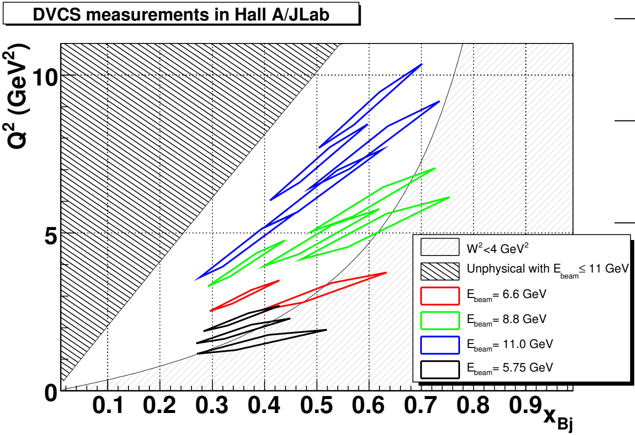

Beam time (days)

Q^2 (GeV^2)	x_{Bj} 0.36	0.50	0.60
3.0	3		
4.0	2		
4.55	1		
3.1		5	
4.8		4	
6.3		4	
7.2		7	
5.1			13
6.0			16
7.7			13
9.0			20
Total	6	20	62

1 GeV^2 range in $t_{min} - t$

88 days

250k events/setting

Physics reach

1. Q^2 variation:
   - 2:1 range at each x_{Bj}
   - Accurate measurement of twist-2 dominance
2. x_{Bj} variation (ξ dependence):
   - Precision data on variation of $t-$dependence with x
   - Study of transverse correlations
3. t variation:
   - 5 bins in $0 < t_{min} - t < 1$ GeV^2
   - Fourier-conjugate to the spatial distributions of quarks as a function of their momentum fraction x
4. π^0 electroproduction cross section:
   - Dominance of Twist-2 (isolation of leading twist)
   - Sensitive to nucleon GPDs $\widetilde{H}$ and $\widetilde{E}$ ($\times$ the π DA)

π^0 electroproduction: $\sigma_L + \sigma_T/\epsilon$

At leading twist:

$$\frac{d\sigma_L}{dt} = \frac{1}{2}\Gamma \sum_{h_N, h_{N'}} |\mathcal{M}^L(\lambda_M = 0, h'_N, h_N)|^2 \propto \frac{1}{Q^6} \qquad \sigma_T \propto \frac{1}{Q^8}$$

$$\mathcal{M}^L \propto \left[\int_0^1 dz \frac{\phi_\pi(z)}{z} \right] \int_{-1}^{1} dx \left[\frac{1}{x-\xi} + \frac{1}{x+\xi} \right] \times \left\{ \Gamma_1 \widetilde{H}_{\pi^0} + \Gamma_2 \widetilde{E}_{\pi^0} \right\}$$

Different quark weights: flavor separation of GPDs

$$|\pi^0\rangle = \frac{1}{\sqrt{2}}\{|u\bar{u}\rangle - |d\bar{d}\rangle\} \qquad \widetilde{H}_{\pi^0} = \frac{1}{\sqrt{2}}\left\{ \frac{2}{3}\widetilde{H}^u + \frac{1}{3}\widetilde{H}^d \right\}$$

$$|p\rangle = |uud\rangle \qquad H_{DVCS} = \frac{4}{9}H^u + \frac{1}{9}H^d$$

Upgrades (from E00-110)

1. Expanded PbF_2 calorimeter: $11\times12+\underline{76}$ blocks.
    - Higher acceptance for π^0 measurements/subtraction.
    - Increased $t-$acceptance: $\Delta(t_{min}-t)=1\,\mathrm{GeV}^2$.
2. Electronics:
    - ARS system (as E00-110) + Upgraded calorimeter trigger (2 thresholds to increase $ep\to ep\pi^0$ statistics).
    - FPGA & VME upgrades to increase livetime & bandwidth.
3. No proton detection: calorimeter can handle $4\times$ E00-110 rate
4. Flared beam pipe to minimize secondary background in calorimeter.
   (Background dominated by Møller and $\pi^0\to\gamma\gamma$ from target)

Experimental configuration $(e\,p \rightarrow e\,\gamma\,X)$

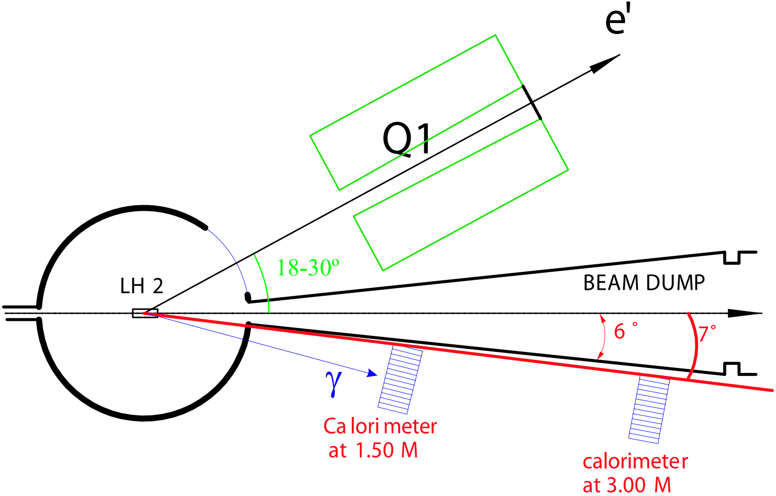

Calorimeter radiation damage

E00-110 experience:

- Dose dominated by e and π^0 above 15° and Møller below 10°
- Dose grows a factor 5 from 11.5° to 7.5°
- 20% gain loss without loss in M_X^2/energy resolution

New experiment strategies:

- Minimum angle of the closest block: 7°
- Luminosity equal to the peak luminosity in E00-110 taking into account the distance to the target: $\mathcal{L} = 4 \cdot 10^{37} (D/110\,\text{cm})^2\,\text{cm}^{-2}\text{s}^{-1}$
- Blue light curing (MAMI-A4): 17 h to cure a transparency loss of 25%

Curing every 6th day of running at the minimum angle

Total of 12 curing days for 88 beam days

Missing mass resolution

(Cf. Table V for all kinematic settings)

6.6 GeV setting

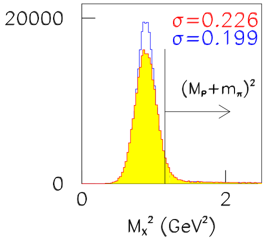

11 GeV setting

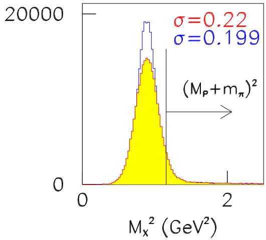

E00-110 **This proposal**

Very similar M_X^2 resolution ⇒ same exclusivity with $e\ \gamma$ *detection only*.

Cross sections

- Model by Vanderhaeghen, Guichon & Guidal (VGG), with factorized $t-$dependence
- 250k events/setting or 40k events per $t-$bin
- Similar statistical accuracy as E00-110

Helicity-independent cross sections (pb/GeV^4)

6.6 GeV setting $Q^2 = 3.0\,\text{GeV}^2$, $x_{\text{Bj}} = 0.36$

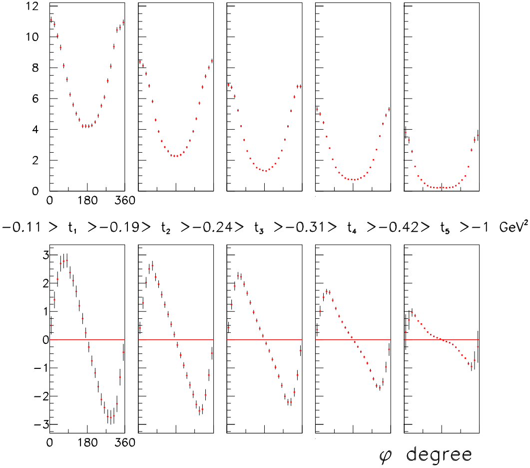

Helicity-dependent cross sections (pb/GeV^4)

Cross sections

Helicity-independent cross sections (pb/GeV^4)

8.8 GeV setting $Q^2 = 4.8\,\mathrm{GeV}^2$, $x_{\mathrm{Bj}} = 0.50$ 11 GeV setting $Q^2 = 9.0\,\mathrm{GeV}^2$, $x_{\mathrm{Bj}} = 0.60$

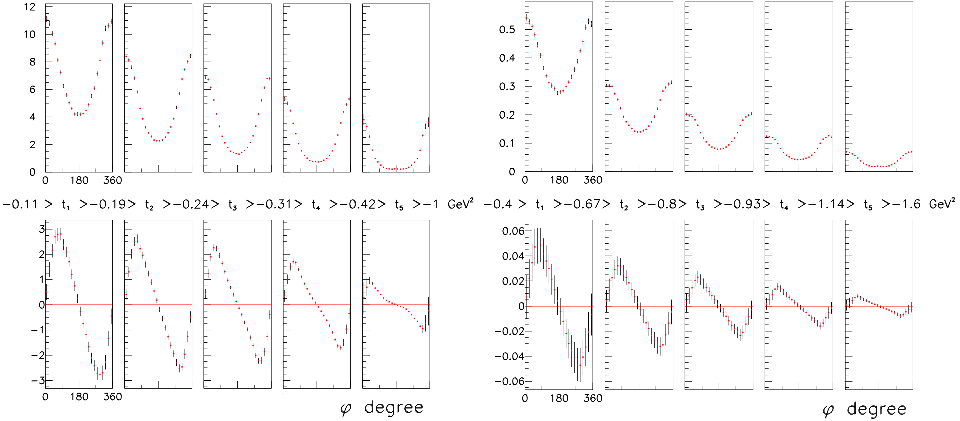

Helicity-dependent cross sections (pb/GeV^4)

Systematic errors

Type		Relative errors (%) E00-110	Relative errors (%) proposed
Luminosity	target length and beam charge	1	1
HRS-Calorimeter	Drift chamber multi-tracks	1.5	1
	Acceptance	2	2
	Trigger dead-time	0.1	0.1
DVCS selection	π^0 subtraction	3	1
	e(p,e'γ)πN contamination	2	3
	radiative corrections	2	1
Total cross section sum		4.9	4.1
Beam	Polarization $\Delta P/P$	2	1
Total cross section difference		5.3	4.2

Model prediction for Q^2, $x_{\rm Bj}$ and t dependencies

- **Sample** of statistical & systematic errors on coefficients
- Total of 55 data points
- Full $t-$dependence at each $(Q^2,x_{\rm Bj})$ point

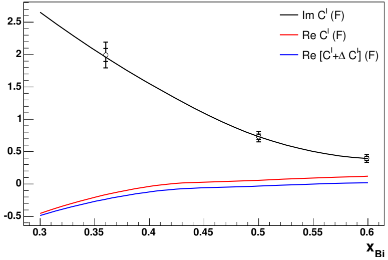

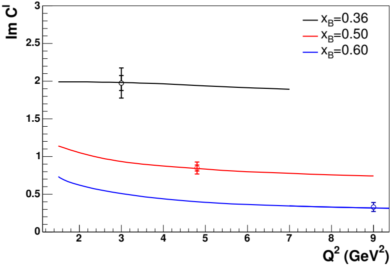

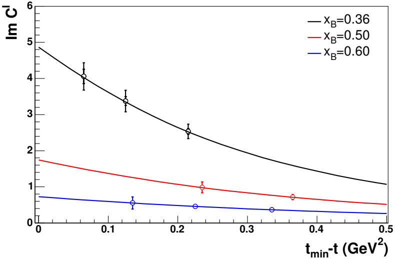

Summary

- **Absolute** DVCS cross sections in almost the complete kinematic region of JLab12
- **Precision** determination of Twist-2 and Twist-3 observables: ξ, t (and Q^2) scan
- π^0 electroproduction **cross sections**

...using the successful experimental technique of E00-110 (nucl-ex/0607029)

This experiment requires 88 days of beam + 12 days for calorimeter curing

Future extentions: DVCS on the neutron, recoil polarimetry...

Supplementary slides

Equipment

- Compton polarimeter
  - LPC-Clermont: equipment & technical manpower
- HRS electronics:
  - LPC-Clermont: pre-trigger electronics
  - ODU: technical manpower for DAQ integration
- PbF_2:
  - LPC-Clermont:
    - Upgrade to trigger & DAQ
    - PMT custom bases & preamps.
  - Other collaborators:
    - 76 additional crystals & PMTs

Recoil polarimetry

- Solenoid (or Helmholtz coil) on the target for high luminosity recoil detection
- Recoil proton polarimetry $H(\vec{e}, e'\gamma\vec{p})$:
  - 7 cm Carbon analyser $\rightarrow$ FoM ($p > 500$ MeV/c) > 0.005
  - Full separation of all four GPDs
- Coherent light nuclei: $D(e, e'\gamma D)$, ${}^{3,4}He(e, e'\gamma\, {}^{3,4}He)$

DVCS on the neutron and deuterium

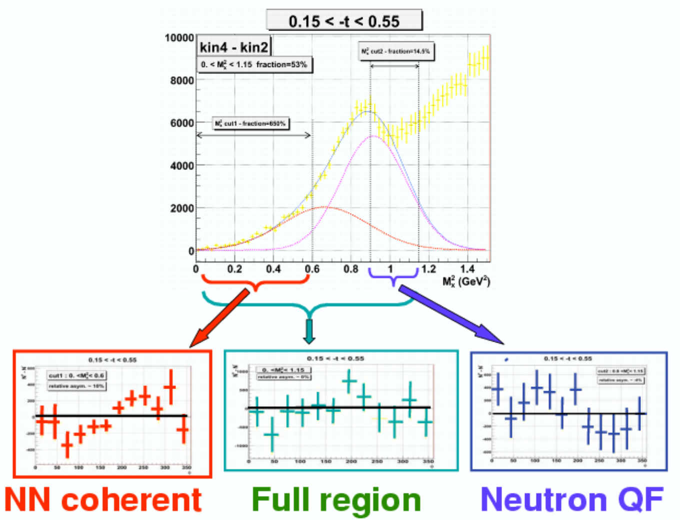

Kinematic constraints

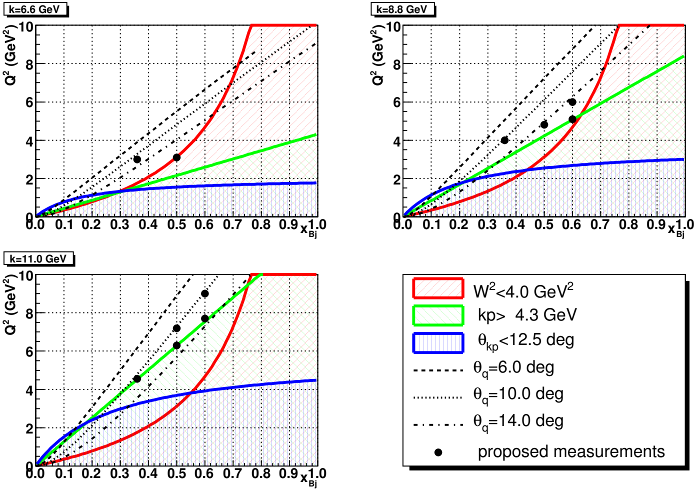

Kinematic settings

Q^2 (GeV^2)	k (GeV)	x_{Bj}	$q'(0°)$ (GeV)	D (m)	θ_q (deg)	θ_{calo}^{min} (deg)	t_{min} (GeV^2)	t_{max} (GeV^2)	$\sigma(M_X^2)$ (GeV^2)	$\mathcal{L}/10^{38}$ (cm^{-2}/s
3.0	6.6	0.36	4.35	1.5	11.7	7.1	-0.16	-0.42	0.23	0.75
4.0	8.8	0.36	5.83	2.0	10.3	7.0	-0.17	-0.42	0.26	1.3
4.55	11.0	0.36	6.65	2.5	10.8	7.0	-0.17	-0.42	0.27	2
3.1	6.6	0.5	3.11	1.5	18.5	11.0	-0.37	-0.64	0.17	0.75
4.8	8.8	0.5	4.91	2.0	14.5	8.9	-0.39	-0.70	0.20	1.3
6.3	11.0	0.5	6.50	2.5	12.4	7.9	-0.40	-0.72	0.20	2.
7.2	11.0	0.5	7.46	2.5	10.2	7.0	-0.40	-0.75	0.25	2.
5.1	8.8	0.6	4.18	1.5	17.8	10.4	-0.65	-1.06	0.16	0.75
6.0	8.8	0.6	4.97	2.0	14.8	9.2	-0.67	-1.05	0.18	1.3
7.7	11.0	0.6	6.47	2.5	13.1	8.6	-0.69	-1.10	0.20	2.
9.0	11.0	0.6	7.62	3.0	10.2	7.3	-0.71	-1.14	0.22	3.
						edge				

§II.D: BH•DVCS & Bilinear-DVCS Terms

$$\frac{d^5\vec{\sigma}(\lambda)}{d^5\Phi} = \frac{d^5\sigma^{BH}}{d^5\Phi}$$

$$+\frac{1}{P_1(\phi)P_2(\phi)}\sum_n \left\{ K^I_{cn}\,\Re e\left[C^I_n\right]\cos(n\phi) + \lambda K^I_{sn}\,\Im m\left[C^I_n\right]\sin(n\phi)\right\}$$

$$+K^{DVCS}_{c0}\Re e\left[\mathcal{C}^{DVCS}(\mathcal{F},\mathcal{F}^*)\right] + \left\{\begin{matrix} K^{DVCS}_{c1} \\ \lambda K^{DVCS}_{s1}\end{matrix}\right\}\left\{\begin{matrix}\cos\phi\,\Re e \\ \sin\phi\,\Im m\end{matrix}\right\}\left[\mathcal{C}^{DVCS}(\mathcal{F}^{eff},\mathcal{F}^*)\right]$$

Twist-2 Twist-3

- Fourier analysis of cross section combines Bilinear terms into effective BH*DVCS observables, with acceptance averaged kinematic weights η_Λ.

$$\eta_{s1} = \left\langle P_1 P_2 K^{DVCS}_{s1} / K^I_{s1} \right\rangle_{acc}$$

$$\eta_{c,i} = \left\langle P_1 P_2 K^{DVCS}_{c,i} / K^I_{c,i} \right\rangle_{acc} \propto \frac{-t x_{Bj}}{Q^2}$$

§II.D: BH•DVCS & Bilinear-DVCS Terms
Effective [Twist-2] Interference Terms

$$\frac{d^5\vec{\sigma}^{\exp}(\lambda)}{d^5\Phi} = \frac{d^5\sigma^{BH}}{d^5\Phi} + \frac{1}{P_1(\phi)P_2(\phi)}\Big[K_0^I\,\Re e\big[C^{I,\exp}(\mathsf{F})\big] + K_0^I\,\Re e\big[C+\Delta C\big]^{I,\exp}(\mathsf{F})$$

$$+\begin{Bmatrix} K_{c1}^{DVCS}\cos\phi \\ \lambda K_{s1}^{DVCS}\sin\phi \end{Bmatrix}\begin{Bmatrix}\Re e\\ \Im m\end{Bmatrix}\Big[C_n^{I,\exp}(\mathsf{F})\Big]\Big]$$

$$\Im m\big[C_1^{I,\exp}\big] = \Im m\big[C^I(\mathsf{F})\big] + \langle\eta_{s1}\rangle\Im m\big[\mathcal{C}^{DVCS}(\mathsf{F}^{eff},\mathsf{F}^*)\big]$$

$$\Re e\big[C^{I,\exp}\big] = \Re e\big[C_0^I(\mathsf{F})\big] + \langle\eta_{c1}\rangle\Re e\big[\mathcal{C}^{DVCS}(\mathsf{F},\mathsf{F}^*)\big] + Twist3$$

$$\Re e\big[(C+\Delta C)^{I,\exp}\big] = \Re e\big[(C+\Delta C)^I(\mathsf{F})\big] + \langle\eta_0\rangle\Re e\big[\mathcal{C}^{DVCS}(\mathsf{F},\mathsf{F}^*)\big] + Twist3$$

E00-110: $\langle\eta_{s1}\rangle \approx -0.1$
$|\langle\eta_0\rangle| \approx |\langle\eta_{c1}\rangle| < 0.051$

$$\eta_\Lambda \propto \frac{-t x_{Bj}}{Q^2}$$

π^0 substraction ($\pi^0 \to \gamma\gamma$)

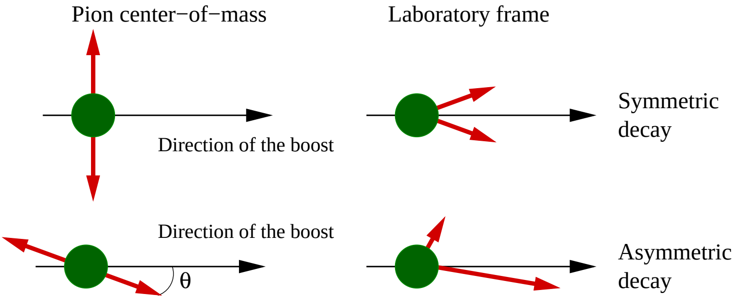

- Symmetric decay: minimum angle in lab of 4.4° for $E_{\pi^0}^{\mathrm{max}} = 3.5\,\mathrm{GeV}$
  $\Rightarrow$ **Clusters separation**
- Asymmetric decay: sometimes only 1-cluster
  $\Rightarrow$ **Mistaken for DVCS event**

π^0 substraction ($\pi^0 \rightarrow \gamma\gamma$)

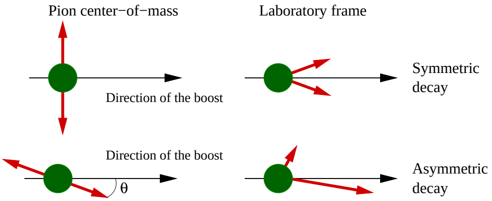

Substraction procedure:

1. Compute kinematics of each *detected* π^0 (2 clusters in calorimeter).
2. Randomize the decay : sample $\cos\theta$ randomly between [-1,1] a big number of times (~ 5000).
3. Compute the ratio of 2-cluster/1-cluster events generated by this π^0 ($\sim$30% in average).

Repeating this procedure for *each* detected π^0 provides an automatic normalization of the contamination as a function of Q^2, t, φ, ...

π^0 subtraction results for different $(t,\, \phi_{\gamma\gamma})$ bins

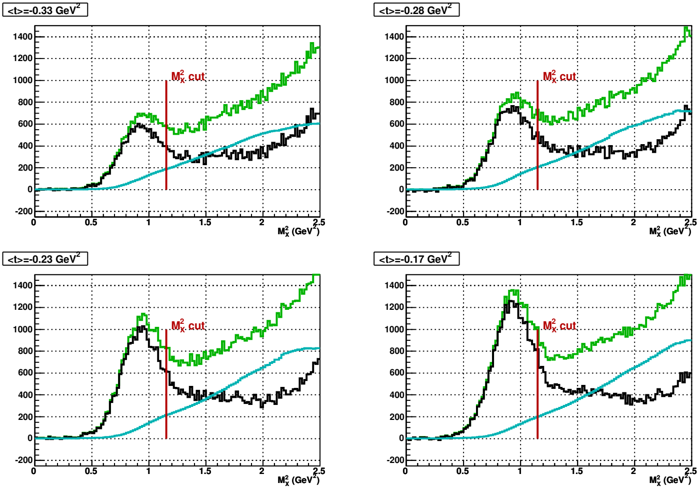

π^0 subtraction results for different $(t, \phi_{\gamma\gamma})$ bins

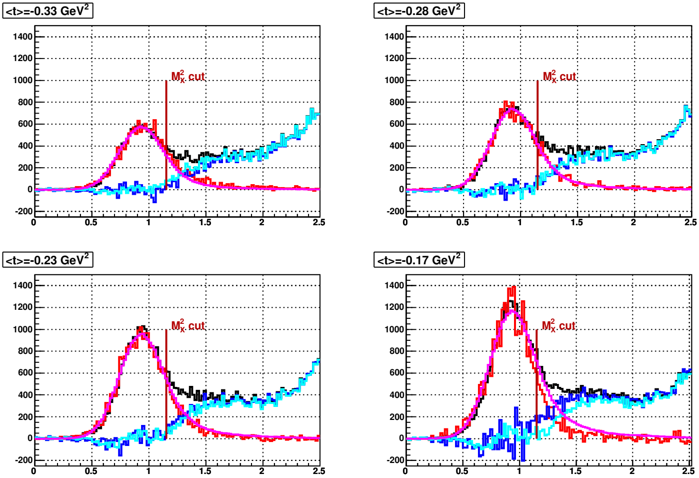

π^0 subtraction results for different $(t, \phi_{\gamma\gamma})$ bins

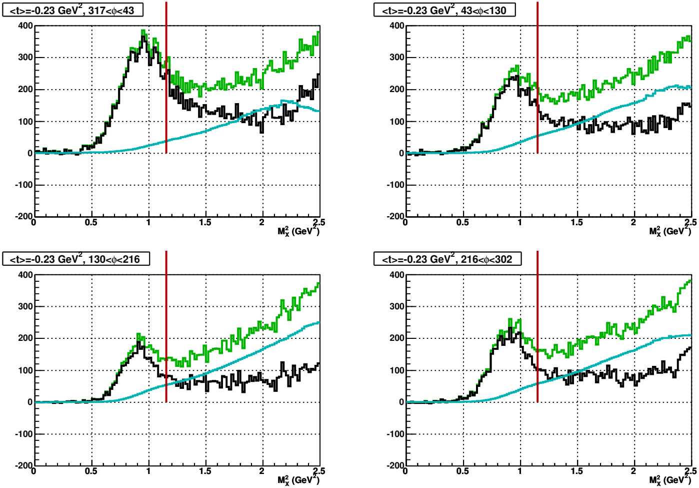

π^0 subtraction results for different $(t,\, \phi_{\gamma\gamma})$ bins

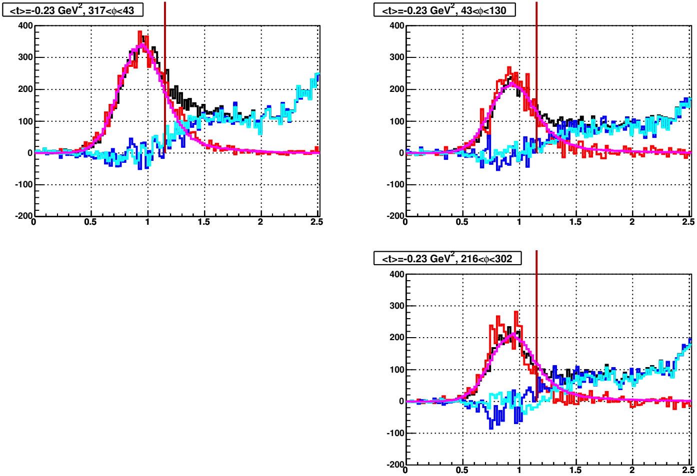

π^0 identification

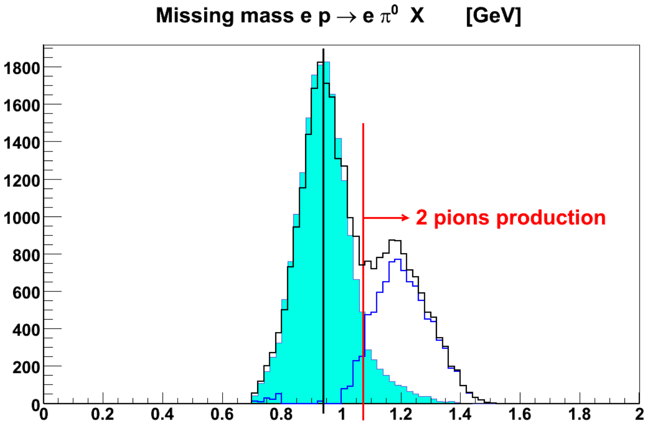

Calorimeter resolution

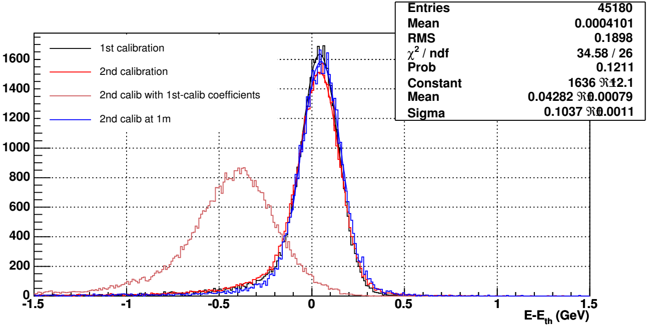

Figure: Energy resolution obtained in both elastic calibration: 2.4%, the average energy of the incident electron being 4.2 GeV. The results of the second calibration when first calibration coefficients are used are also plotted to show the necessity of a careful monitoring of the coefficients in between these two calibration points.

Calibration coefficients evolution

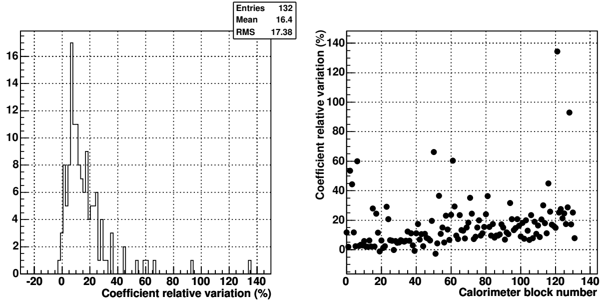

Figure: Relative variation of the calorimeter calibration coefficients between two elastic calibration. Their values are histogrammed (left) and plotted as a function of the block number (right). Larger block numbers correspond to blocks closer to the beamline. These blocks have accumulated a larger radiation dose and their gain have decreased more than those of other blocks.